Qualitative and Quantitative Phase-Analysis of Undoped Titanium Dioxide and Chromium Doped Titanium Dioxide from Powder X-Ray Diffraction Data

Hari Sutrisno[1,*], Ariswan[2], and Dyah Purwaningsih[1]

[1]*Department of Chemistry Education, Faculty of Mathematics and Natural Sciences, Universitas Negeri Yogyakarta (UNY), Jl. Colombo No.1, Yogyakarta 55281, Indonesia*

[2]*Department of Physics Education, Faculty of Mathematics and Natural Sciences, Universitas Negeri Yogyakarta (UNY), Jl. Colombo No.1, Yogyakarta 55281, Indonesia*

ABSTRACT

Undoped titanium dioxide (TiO_2) and a series of chromium(III) doped TiO_2 (Cr-doped TiOfig. 1₂) with various %wt Cr atom were prepared by a reflux technique. The undoped TiO_2 and Cr-doped TiO_2 of 1.1, 3.9, 4.4 %wt Cr atom have been successfully analyzed both qualitative and quantitative analysis of powder X-ray diffraction (XRD) data. The qualitative analysis was carried out with the identification of phases in all samples by comparison with Crystallography Open Database (COD) and International Centre for Diffraction Data (ICDD), while the quantitative phase analysis was calculated by reference intensity ratio (RIR) and whole-pattern fitting (Rietveld analysis) methods. The undoped TiO_2 consist of three phases: anatase, rutile, and brookite. In the 1.1 %wt Cr-doped TiO_2 are detected presenting two phases: anatase (major) and rutile (minor). In the 3.9 %wt Cr-doped TiO_2 and in the 4.4 %wt Cr-doped TiO_2 consist of anatase as major phase, while CrO_2 and TiO_2-II phases can be detected as minor phases. The undoped TiO_2 was refined in the phase, crystal system and space group of anatase (tetragonal, $I4_1/amd$), rutile (tetragonal, $P4_2/mnm$) and brookite (orthorhombic, $Pbca$), while the 1.1 %wt Cr-doped TiO_2 was refined based on anatase (tetragonal, $I4_1/amd$), rutile (tetragonal, $P4_2/mnm$). Finally, in the 3.9 %wt Cr-doped TiO_2 and 4.4 %wt Cr-doped TiO_2, respectively were refined in the crystal system and space group of anatase (tetragonal, $I4_1/amd$).

Keywords: *titanium dioxide; Rietveld analysis; X-ray powder diffraction*

ABSTRAK

Titanium dioksida (TiO_2) dan TiO_2 terdadah variasi % berat Cr(III) berhasil dipreparasi dengan teknik refluks. Titanium dioksida dan TiO_2 terdadah 1,1; 3,9; dan 4,4% berat atom Cr dianalisis secara kualitatif dan kuantitatif dari data difraksi sinar-X (XRD) serbuk. Analisis kualitatif dilakukan dengan cara mencocokkan data pola XRD sampel dengan data pola XRD standard dari Crystallography Open Database (COD) dan International Centre for Diffraction Data (ICDD). Analisis kuantitatif dihitung berdasarkan metode "reference intensity ratio" (RIR) and "whole-pattern fitting" (metode Rietveld). Sampel TiO_2 berisi tiga fasa kristal: anatas, rutil, dan brookit, sedangan TiO_2 terdadah 1,1% berat atom Cr mengandung dua fasa: anatas (utama) dan rutil (minor). Masing-masing, pada TiO_2 terdadah 3,9% berat atom Cr dan TiO_2 terdadah 4,4% berat atom Cr terkandung anatas sebagai fasa utama, sedangkan fasa CrO_2 dan TiO_2-II hadir dalam jumlah sangat sedikit. Penghalusan Rietveld pada TiO_2 dilakukan dengan berdasarkan atas fasa, sistem kristal dan kelompok ruang: anatas (tetragonal, $I4_1/amd$), rutil (tetragonal, $P4_2/mnm$) dan brookit (ortorombik, $Pbca$), sedangkan pada TiO_2 terdadah 1,1% berat atom Cr dilakukan penghalusan berdasar atas sistem kristal dan kelompok ruang: anatas (tetragonal, $I4_1/amd$) and rutil (tetragonal, $P4_2/mnm$). Akhirnya, penghalusan struktur pada TiO_2 terdadah 3,9% berat atom Cr dan pada TiO_2 terdadah 4,4% berat atom Cr dilaksanakan berdasar atas sistem kristal dan kelompok ruang: anatas (tetragonal, $I4_1/amd$).

Kata Kunci: *titanium dioksida; analisis Rietveld; difraksi sinar-X serbuk*

INTRODUCTION

Titanium dioxide (titania, TiO_2) is the most commonly employed of the n-type semiconductors due to its high photoactivity and stability, relatively low cost, and non-toxicity. TiO_2 is widely employed in various applications, especially in photocatalyst [1-3], antibacterial [4-6] and photovoltaic devices [7-9], super-hydrophilic and light-induced amphiphilic surfaces [10-12].

Titanium dioxide has eleven different structure phases (allotropes): anatase, rutile, brookite, $TiO_2(B)$, $TiO_2(H)$-hollandite, $TiO_2(R)$-ramsdellite, TiO_2-columbite (α-PbO_2 type, TiO_2-II), TiO_2-baddeleyite (TiO_2-MI), TiO_2-orthorhombic (TiO_2-OI), TiO_2-fluorite (CaF_2 type), and TiO_2-cotunnite. Three of these crystalline forms of TiO_2 occur in nature as mineral: anatase (tetragonal, $I4_1/amd$) [13], rutile (tetragonal, $P4_2/mnm$) [13], and brookite (orthorhombic, $Pbca$) [14], but only rutile and anatase have been able to be synthesized in pure form at low temperature until recent days.

A semiconductor is characterized by the presence of band energetic structure, with a band gap between the lower, valence band (VB) and the higher energetic, conduction band (CB). Electrons present in the occupied band (VB) are photoexcited and move to the CB, leaving a positive charged hole (h^+), when the semiconductor is photo-irradiated by light with photon energy (hv) at least equal to the band gap. Once formed, the electron (e^-) and hole (h^+) pair may undergo either fast recombination. A photocatalytic reaction will occur that leads to the development of useful processes. Anatase shows a band gap of 3.2 eV, corresponding to a UV wavelength adsorption of 387 nm [15]. In contrast, rutile has a smaller band gap (3.0 eV), with excitation wavelengths that extend into the visible light range (410 nm) [16] and the band gap of the metastable brookite is 3.54 eV [17]. Many metal ions are used as dopant to increase the λ radiation adsorption, such as niobium [18], argentum [19-20], vanadium [21], ferrum [22], zinc [23], and chromium [24-26].

X-ray diffraction is the most useful technique for qualitative and quantitative phase analysis in multi-phase. Qualitative analysis identifies phases in a specimen compared to "standard" patterns such as American Society for Testing and Materials (ASTM), Joint Committee on Powder Diffraction Standards (JCPDS), Crystallography Open Database (COD), Inorganic Crystal Structure Database (ICSD) and International Centre for Diffraction Data (ICDD). X-ray diffraction pattern gives information about peak positions, intensity, and shape. Qualitative analysis of powder diffraction data is the identification of crystal phase, peak position and intensity related to unique crystal structure. Quantitative analysis of powder diffraction data refers to the determination of amounts of different phases in multi-phase samples. Quantification can be carried out because the intensity of the diffraction pattern of a phase or phases in a mixture depends on its concentration. There are several methods of X-ray diffraction to quantify phases such as direct comparison, internal standard, external standard, absorption-diffraction, reference intensity ratio (RIR) and whole-pattern fitting (Rietveld analysis) [27-30].

The objectives of this research are (1) qualitative phase analysis in undoped titanium dioxide and a series of chromium doped TiO_2 compared to "standard" patterns: COD and ICDD, (2) analysis of quantitative phase in the samples by comparing two methods: RIR and whole-pattern fitting (Rietveld analysis). This research is important to know the precise and accurate method of qualitative and quantitative analysis in determining the crystalline phases contained in a sample of Cr doped TiO_2 solid solutions.

EXPERIMENTAL SECTION

Materials

Ammonium hydroxide (NH_4OH, 28-30% NH_3) solution, hydrogen peroxide (H_2O_2, 10 %wt in H_2O), ammonium chromate ($(NH_4)_2CrO_4$, 99%), titanium (IV) chloride ($TiCl_4$, 99%) were purchased from Sigma-Aldrich. All the reagents were used without further purification. Titanium dioxide hydrate ($Ti(O_2)O.2H_2O$) was obtained from the reaction of $TiCl_4$ and H_2O_2 [31]. A series of chromium(III) doped TiO_2 with various %wt Cr atom were prepared by the reflux technique. In a typical synthesis, 10 g $Ti(O_2)O.2H_2O$ is dissolved in 50 mL of distilled water under vigorous stirring. The solution was kept stirring for 4 h to obtain colloid A. In order to investigate the effect of the $(NH_4)_2CrO_4$ concentration, in a separated beaker 0, 3, 6, and 9 %wt Cr-doped TiO_2 respectively were adopted. It was dissolved in 20 mL of distilled water thoroughly under vigorous stirring to obtain solution B1, B2, B3, and B4, respectively. Each solution B1, B2, B3 and B4 was then slowly added to each solution A. The final solution mixture was sealed and further stirred for 2 h, then added dropwise NH_4OH until pH $\approx$ 8-10. Finally the solution is heated with a magnetic stirrer in equipment reflux at 150 °C for 6 h. Precipitate is filtered, washed with distilled water and dried at 70 °C for 3 h. Furthermore, the precipitate was calcined at 600 °C for 2 h.

Instrumentation

In order to obtain XRD powder data, a Rigaku Miniflex 600-Benchtop diffractometer with a copper tube and Kα radiation of λ = 1.5406 Å, operating at 40 kV and 15 mA, was used. The samples were mounted in a silica glass sample holder. The powder XRD data were collected in the 2θ interval ranging from 2° to 90° with a step width of 0.02° and a counting time of 5 sec/step.

Scanning electron microscope (Phenom ProX Desktop SEM) equipped with energy dispersive X-ray spectroscopy (EDS) was used to analyze the presence

of Ti and O elements in the TiO_2 and the presence of Ti, Cr, and O elements in the Cr-doped TiO_2.

Procedure

Qualitative phase analysis

Diffraction patterns are unique "fingerprints" of the crystal structure of materials that can be used to determine phase composition of a polycrystalline material. Phase identification is essentially an exercise of pattern comparison between the unknown and a database of single-phase reference patterns. The qualitative analysis was carried out with the identification of a phase or phases in the samples by comparison with "standard" patterns: COD and ICDD.

Quantitative phase analysis

Quantitative analysis of diffraction data usually refers to the determination of amounts of different phases in multi-phase samples. The quantitative phase analysis was calculated by comparing two methods: reference intensity ratio (RIR) and whole-pattern fitting (Rietveld analysis).

Reference Intensity Ratio (RIR) method. The RIR is a method used for quantitative analysis by powder diffraction and is based upon scaling all diffraction data to the diffraction of standard reference materials. The RIR method can be used to determine concentrations by using ratios and measuring peak areas. Klug and Alexander were first to describe a technique for quantification using intensities of the crystalline phases in a mixture as in equation 1 [27]:

$$\frac{I_{(hkl)A}}{I_{(hkl)B}} = k \frac{X_A}{X_B} \qquad (1)$$

where, ratio of peak intensity from *unknown* phase 'A' ($I_{(hkl)}$) to a *standard* 'B' ($I_{(hkl)}$) is a linear function of the mass fraction of 'A' in the original sample and the amount of minerals in known internal standards (eg, rutile, silica) is used to calibrate unknown phase intensities.

ICDD PDF-2 uses corundum (Al_2O_3) as reference B and gives k for 50:50 mixtures of phase A and corundum. RIR is I/I_{cor} using intensity of the strongest peak (100%), If I_1/I_{cor} is k_1 and I_2/I_{cor} is k_2, then I_1/I_2 is k_1/k_2. The RIR values or intensity ratio of the more intense peak of each phase respect to the (113) peak of corundum reported in the PDF of the ICDD is expressed as (2) [32]:

$$w_1 = \frac{I_1^k \, w_{corrundum}}{I_{corrundum}^{113} \, RIR_{1,corrundum}} \qquad (2)$$

where, w_1 = weight fraction of phase 1 and $w_{corrundum}$ = weight fraction of corundum.

Whole-pattern fitting method (Rietveld analysis).

Rietveld (1969) developed a method to refine crystal structure information using neutron powder diffraction [32]. The Rietveld method is based on a least-squares fit between step-scan data of a measured diffraction pattern and a simulated X-ray-diffraction pattern. The simulated XRD pattern is calculated from a large number of parameters, including crystal-structure parameters of each component phase, a scale factor for each constituent phase to adjust the relative intensities of the reflections, parameters describing the peak profile and the background, and parameters simulating the instrumental aberrations as well as effects resulting from size-related strain, preferred orientation, and particle size. A key feature of the quantitative analysis of phase proportions by the Rietveld method is that the phase abundances of the constituent phases can be directly calculated from the refined scale-factors. To refine each XRD spectrum in the research, The Rietveld analysis was applied by using Fullprof software by Roisnel and Rodriguez Carbajal on the package WinPlotr [33]. In the refinement procedure, a calculated pattern is fitted to an observed diffraction pattern by the least-squares method, until the best fit is obtained. The least-squares refinement leads to a minimal residual quantity (χ^2) in the Rietveld Method [34] is,

$$\chi^2 = \sum_{i=1}^n w_i \left\{ y_i - y_{c,i}(\alpha) \right\}^2 \qquad (3)$$

with $w_i = 1/\sigma_i^2$, being σ_i^2 the variance of the "observation" y_i, y_i = observed intensity at the ith step, and $y_{c,i}$ = calculated intensity at the ith step. The calculated profile of X-ray powder pattern can be well described by the equation:

$$y_{c,i} = \sum_\phi S_\phi \sum_h I_{\phi,h} \Omega \left(T_i - T_{\phi,h} \right) + b_i \qquad (4)$$

In Fullprof, the term phase is synonymous of a same procedure for calculating the integrated intensities ($I_{\phi,h}$). Rietveld phase quantification (sometimes called also standardless phase analysis, multiphase Rietveld quantitative analysis or Rietveld XRD quantification) is a powerful method for determining the quantities of crystalline and amorphous components in multiphase mixtures. The weight fraction (W_i) for each phase was obtained from the refinement relation [34]:

$$W_i = \frac{S_i (ZMV)_i}{\sum_j S_j (ZMV)_j} \qquad (5)$$

where i is the value of j for a particular phase among the N phases present. The S, Z, M, and V are, respectively, the Rietveld scale factor, the number of
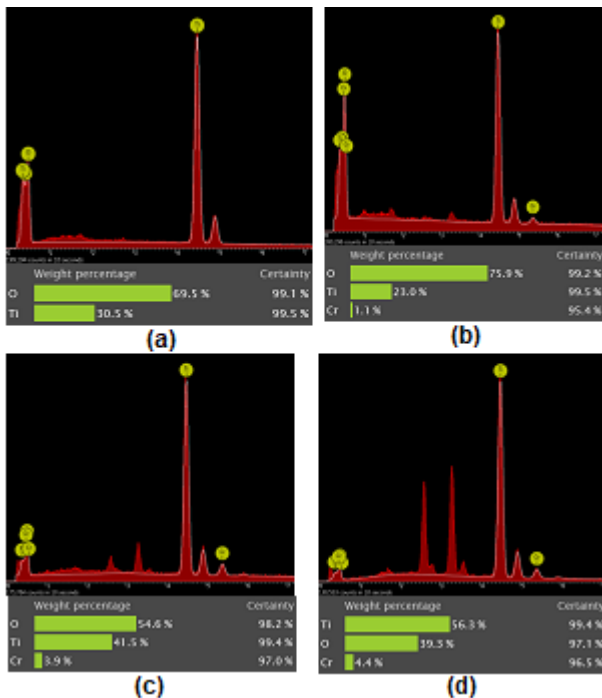
Fig 1. EDS analysis and weight percentage of Ti, O and Cr of (a). undoped TiO_2, (b). 1.1 %wt Cr-doped TiO_2, (c). 3.9 %wt Cr-doped TiO_2, and (d). 4.4 %wt Cr-doped TiO_2

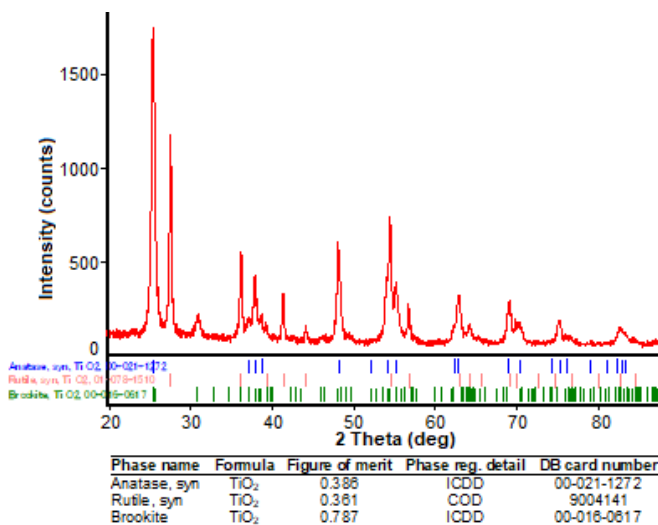| Phase name	Formula	Figure of merit	Phase reg. detail	DB card number
Anatase, syn	TiO_2	0.386	ICDD	00-021-1272
Rutile, syn	TiO_2	0.361	COD	9004141
Brookite	TiO_2	0.787	ICDD	00-016-0617

Fig 2. XRD diagram and the result of qualitative analysis of undoped TiO_2

formula units per cell, the mass of the formula unit (in atomic mass units) and the unit cell volume (in Å^3). The fit must be evaluated by visual comparison between the observed and calculated pattern. The quality of the agreement between observed and calculated profiles is measured by a set of nowadays-conventional factors (profile factor (R_p), weighted profile factor (R_{wp}), expected
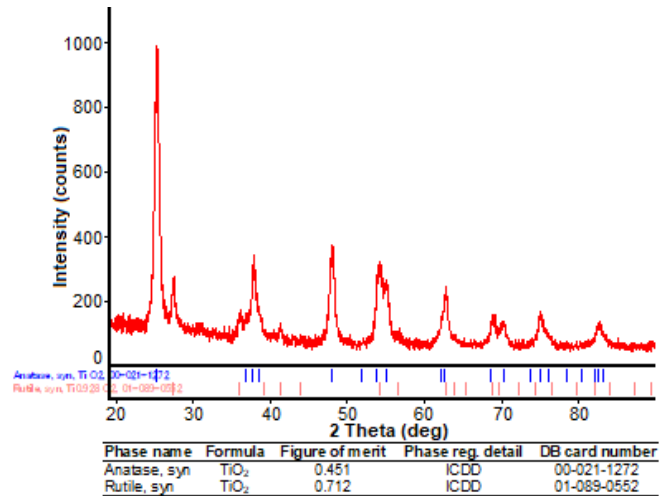

Phase name	Formula	Figure of merit	Phase reg. detail	DB card number
Anatase, syn	TiO_2	0.451	ICDD	00-021-1272
Rutile, syn	TiO_2	0.712	ICDD	01-089-0552

Fig 3. XRD diagram and the result of qualitative analysis of 1.1 %wt Cr-doped TiO_2

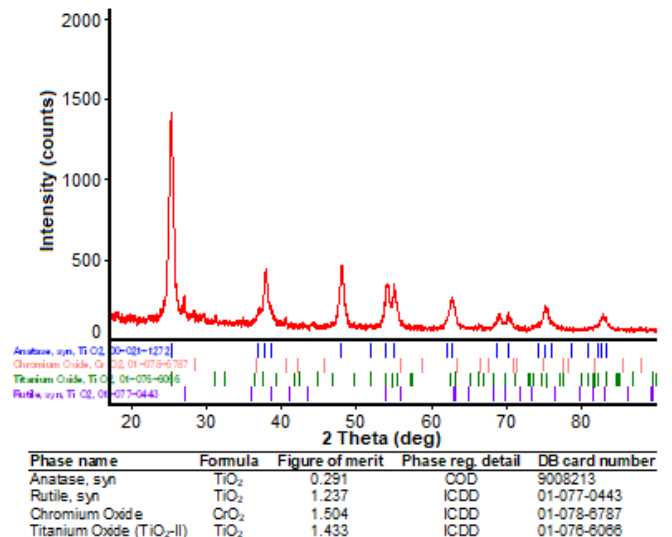| Phase name	Formula	Figure of merit	Phase reg. detail	DB card number
Anatase, syn	TiO_2	0.291	COD	9008213
Rutile, syn	TiO_2	1.237	ICDD	01-077-0443
Chromium Oxide	CrO_2	1.504	ICDD	01-078-6787
Titanium Oxide (TiO_2-II)	TiO_2	1.433	ICDD	01-076-6066

Fig 4. XRD diagram and the result of qualitative analysis of 3.9 %wt Cr-doped TiO_2

weighted profile Ffactor (R_{exp}), and goodness of fit indicator (GoF)).

RESULT AND DISCUSSION

EDS Analysis

The scanning electron microscopy-energy dispersive X-ray spectroscopy (SEM-EDS) analysis reveals the presence of Ti and O elements in undoped TiO_2 and of Ti, Cr, O elements in various %wt Cr-doped TiO_2. On the theoretical, addition of each: 3, 6 and 9 %wt Cr-doped TiO_2 produced experimentally only 1.1, 3.9 and 4.4 %wt Cr-doped TiO_2 respectively (Fig. 1).

Based on the composition of the atoms, the molecular formula of solid solutions ($Ti_{1-x}Cr_xO_2$) for 1.1, 3.9 and 4.4 %wt Cr-doped TiO2 are $Ti_{0.983}Cr_{0.017}O_2$, $Ti_{0.940}Cr_{0.060}O_2$, and $Ti_{0.932}Cr_{0.068}O_2$, respectively.

Qualitative Phase Analysis

Fig. 2, 3, 4 and 5 show XRD patterns of undoped TiO2 and Cr-doped TiO2 at various %wt Cr atom. All XRD patterns exhibit strong diffraction peaks at 2θ: 25.36, 37.84, 48.11, 54.38, 55.07, and 62.88° indicating TiO2 of anatase phase and at 2θ: 27.53, 36.14, 41.32, and 54.38 indicating TiO2 of rutile phase. The main diffraction peaks are indexed as the (101), (103), (200), (105), (211), (213) reflections of crystalline anatase phase, corresponding to those shown in the ICDD card No. 00-021-1272 and the main diffraction peaks are indexed as the (110), (101), (200), (111), (211) reflections of crystalline rutile phase, corresponding to those shown in the COD card No. 9004141. In the undoped TiO2, there are three phases: anatase, rutile, and brookite (Fig. 2). Fig. 3 shows that the 1.1 %wt Cr-doped TiO2 sample is detected presenting two phases of TiO2: anatase (major) and rutile (minor). In the 3.9 %wt Cr-doped TiO2 (Fig. 4)

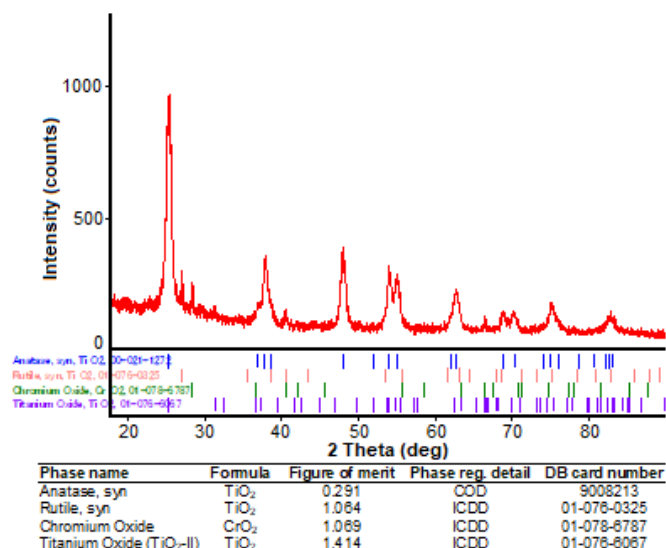and the 4.4 %wt Cr-doped TiO2 (Fig. 5) show the presence of anatase (major), rutile (minor), chromium

Phase name	Formula	Figure of merit	Phase reg. detail	DB card number
Anatase, syn	TiO2	0.291	COD	9008213
Rutile, syn	TiO2	1.064	ICDD	01-076-0325
Chromium Oxide	CrO2	1.069	ICDD	01-078-6787
Titanium Oxide (TiO2-II)	TiO2	1.414	ICDD	01-076-6067

Fig 5. XRD diagram and the result of qualitative analysis of 4.4 %wt Cr-doped TiO2

Table 1. Phase content of TiO2 and (hkl) in undoped TiO2 and various %wt Cr-doped TiO2

Samples				(hkl) planes				
Undoped TiO2	1.1 %wt Cr-doped TiO2	3.9 %wt Cr-doped TiO2	4.4 %wt Cr-doped TiO2	Anatase	Rutile	Brookite	CrO2	TiO2-II
25.36	25.29	25.31	25.33	(101)		(210)		(110)
	27.10	27.06					(011)	
27.53	27.39				(110)			
	28.39	28.39					(110)	
30.95		31.24	31.29			(211)		(111)
36.14	36.04				(101)			
37.05		36.90	36.94	(103)				
37.84	37.76			(004)				
38.04	37.80	37.82	37.93			(311)		
38.67				(112)		(220)		
39.24					(200)	(400)		
	40.54	40.43					(020)	
41.32	41.34				(111)			
44.13					(210)			
48.11	48.00	48.01	48.01	(200)				
	53.98	53.99	53.96			(402)		
54.38				(105)	(211)			
55.07	55.10	55.04	55.02	(211)				
56.63					(220)			
62.88	62.79	62.75	62.72	(213)	(002)			
64.13					(310)	(023)		
			66.38					(023)
68.96	68.87	68.95	68.77	(116)	(301)			
69.85					(112)			
70.34	70.19	70.20	70.08	(220)				
75.06	74.94	75.04	75.02	(215)				
75.98				(301)				
82.54	82.57	82.78	82.63	(224)	(321)	(440)		

Table 2. Phase content of TiO₂ in undoped TiO₂ and various %wt Cr-doped TiO₂ calculated using RIR method

Samples	Phase (%)				
	Anatase	Rutile	Brookite	CrO₂	TiO₂-II
UndopedTiO₂	52.2	25.1	22.7	-	
1.1 %wt Cr-doped TiO₂	87.0	13.0	-	-	
3.9 %wt Cr-doped TiO₂	91.0	2.8	-	2.7	3.3
4.4 %wt Cr-doped TiO₂	96.0	2.2	-	1.4	0.4
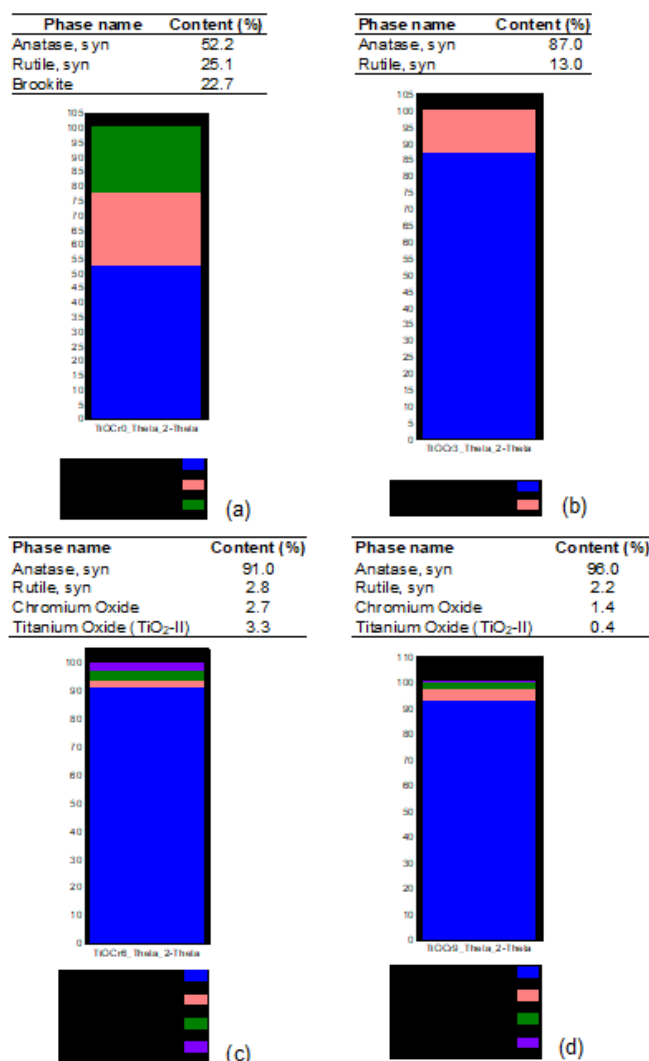
Fig 6. Composition XRD diagram of (a). undoped TiO₂, (b). 1.1 %wt Cr-doped TiO₂, (c). 3.9 %wt Cr-doped TiO₂, and (d). 4.4 %wt Cr-doped TiO₂

oxide (minor) and TiO₂-II (minor). The results of identification of a phase or phases and (hkl) in the samples are showed in Table 1.

Quantitative Phase Analysis

RIR method

Fig. 6 shows the weight fraction of TiO₂ phases calculated using the RIR method. The phase content of all samples calculated by RIR method are showed in Table 2. In the undoped TiO₂ shows the following phase compositions: anatase (52.2%), rutile (25.1%) and brookite (22.7%), while in the 1.1 %wt Cr-doped TiO₂, its phase composition are anatase (87.0%) and rutile (13.0%). The chromium oxide, rutile and TiO₂-II present in the 3.9 %wt Cr-doped TiO₂ and the 4.4 %wt Cr-doped TiO₂, respectively. In the 3.9 %wt Cr-doped TiO₂ are detected 91.0% of anatase, 2.8% of rutile, 2.7% of CrO₂, and 3.3% of TiO₂-II, while in the 4.4 %wt Cr-doped TiO₂ consist of 96.0% of anatase, 2.2% of rutile, 1.4% of CrO₂, and 0.4% of TiO₂-II.

Whole-pattern fitting method (Rietveld analysis)

X-ray diffraction-Rietveld refinement was carried out with the method supplied by the Fullprof software to undoped TiO₂ and various %wt Cr-doped TiO₂. The results of Rietveld refinement are shown in Fig. 7, 8, 9 and 10. The experimental points are given as dot (.) and theoretical data (calculated by eq. (3)) are shown as solid line. Difference between experimental data and theoretical is shown as bottom line. The vertical lines represent the Bragg's allowed peaks. In the undoped TiO₂ were refined in the crystal system and space group of anatase (tetragonal, $I4_1/amd$), rutile (tetragonal, $P4_2/mnm$) and brookite (orthorhombic, $Pbca$) (Fig. 7). No reflections of anatase (major) and rutile (minor) phases are observed in the 1.1 %wt Cr-doped TiO₂ (fig. 8) and it's were refined in the crystal system and space group of anatase (tetragonal, $I4_1/amd$), and rutile (tetragonal, $P4_2/mnm$). In the 3.9 %wt Cr-doped TiO₂ and 4.4 %wt Cr-doped TiO₂ respectively consist of anatase phase, while rutile, chromium dioxide and TiO₂-II phases can't be detected by Rietveld refinements. Fig. 9 and 10 depict Fullprof Pattern Matching of anatase phase in the 3.9 %wt Cr-doped TiO₂ and 4.4 %wt Cr- doped TiO₂ respectively. The results of crystal system, cell parameters (a, b, c) and atomic position (x, y, z) are presented in Table 3.

Fig. 11 shows the relationship between cell volumes of anatase at various %wt Cr atom of Cr-doped TiO₂. The cell volume of anatase crystals have increased with increasing %wt Cr atoms of Cr doped TiO₂. This is due to the replacement of Ti(IV) ions which have crystal radii of 0.746 Å replaced by Cr(III) ions having larger crystal radii that is 0.755 Å [35].

Table 3. The crystal system, cell parameters (a, b, c) and atomic position (x, y, z) of TiO_2 phases in undoped TiO_2 and various %wt Cr-doped TiO_2 calculated by Rietveld method

| Samples	Phase	a (Å)	b (Å)	c (Å)	V (Å³)	Atom	x	y	z
Undoped TiO_2	Anatase Tetragonal, $I4_1/amd$)	3.7819	3.7819	9.5008	135.89	Ti^{+4}	0.0000	0.0000	0.5000
						O^{-2}	0.0000	-0.5000	0.5447
	Rutile (Tetragonal, $P4_2/mnm$)	4.5901	4.5901	2.9553	62.26	Ti^{+4}	0.0000	0.0000	0.0000
						O^{-2}	0.3064	0.3064	0.0000
	Brookite (Orthorhombic, $Pbca$)	9.1601	5.4291	5.1476	255.99	Ti^{+4}	0.1292	0.0912	0.8658
						O_1^{-2}	0.0331	0.1830	0.1427
						O_2^{-2}	0.2136	0.0949	0.5469
1.1 %wt Cr-doped TiO_2	Anatase (Tetragonal, $I4_1/amd$)	3.7930	3.7930	9.5075	136.78	Ti^{+4}	0.0000	0.0000	0.5000
						O^{-2}	0.0000	-0.5000	0.5447
	Rutile (Tetragonal, $P4_2/mnm$)	4.5925	4.5925	2.9574	62.37	Ti^{+4}	0.0000	0.0000	0.0000
						O^{-2}	0.3041	0.3041	0.0000
3.9 %wt Cr-doped TiO_2	Anatase (Tetragonal, $I4_1/amd$)	3.7978	3.7978	9.5205	137.32	Ti^{+4}	0.0000	0.0000	0.5000
						O^{-2}	0.0000	-0.5000	0.5405
4.4 %wt Cr-doped TiO_2	Anatase (Tetragonal, $I4_1/amd$)	3.7972	3.7972	9.5159	137.21	Ti^{+4}	0.0000	0.0000	0.5000
						O^{-2}	0.0000	-0.5000	0.5347
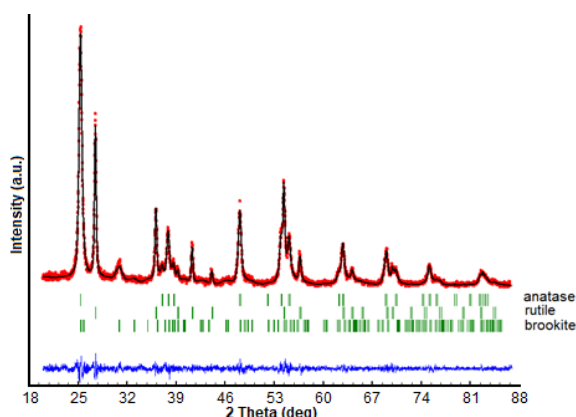
Fig 7. X-ray diffraction Fullprof Patern Matching of undoped TiO_2
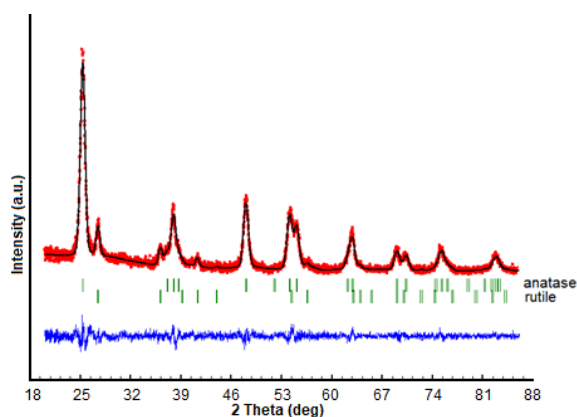
Fig 8. X-ray diffraction Fullprof Patern Matching of 1.1 %wt chromium doped TiO_2
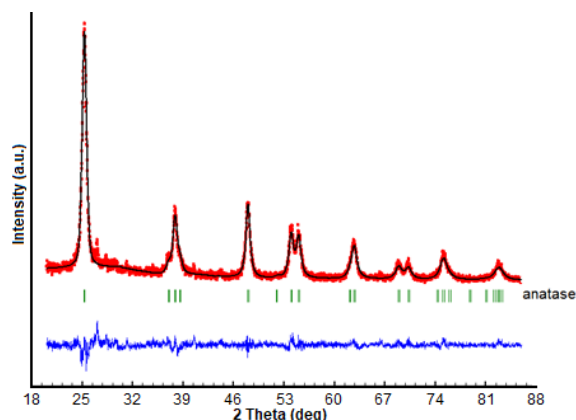
Fig 9. X-ray diffraction Fullprof Patern Matching of 3.9 %wt chromium doped TiO_2
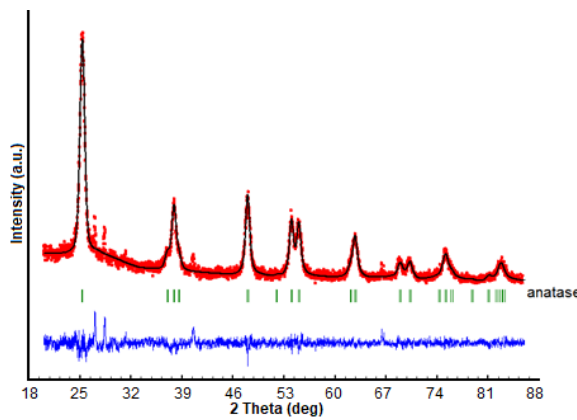
Fig 10. X-ray diffraction Fullprof Patern Matching of 4.4 %wt chromium doped TiO_2

Table 4. Phase content of TiO_2 in undoped TiO_2 and various %wt Cr-doped TiO_2 calculated using Rietveld method

Samples	Phase (%)					R_P (%)	R_{wp} (%)	R_{exp} (%)	GoF
	Anatase	Rutile	Brookite	CrO_2	TiO_2-II				
Undoped TiO_2	49.58	38.39	12.03	-	-	7.02	9.06	8.37	1.08
1.1 %wt Cr-doped TiO_2	88.45	11.50	-	-	-	7.53	9.72	9.43	1.03
3.9 %wt Cr-doped TiO_2	100.00	-	-	-	-	7.84	10.30	8.69	1.18
4.4 %wt Cr-doped TiO_2	100.00	-	-	-	-	8.20	11.10	8.88	1.25
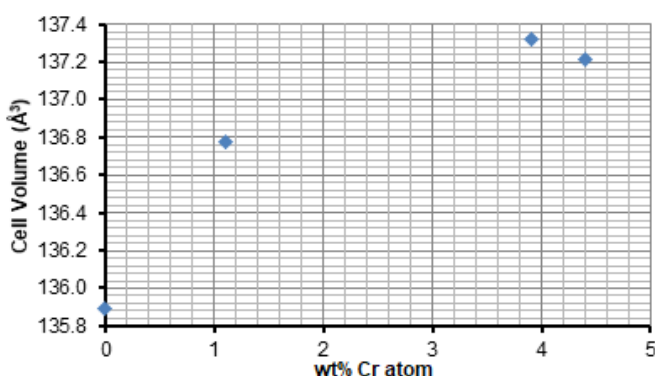
Fig 11. Cell volume of anatase at various %wt Cr atom of Cr-doped TiO_2

The weight percentages of the phases were calculated by using the Rietveld method with the Fullprof software. Quantitative phase analysis obtained by Rietveld analysis by eq. (5). By the Rietveld refinement, the undoped TiO_2 shows the following phase compositions: anatase (49.58%), rutile (38.39%) and brookite (12.03%), while in the 1.1.%wt Cr-doped TiO_2, its phase composition are anatase (88.45%) and rutile (11.50%). In the 3.9 %wt Cr-doped TiO_2 and 4.4 %wt Cr-doped TiO_2 respectively consist of 100% of anatase phase, while rutile, chromium dioxide and TiO_2-II phases can't be refined by Rietveld analysis. According to these results and the quality of the agreement between observed and calculated profiles, it can be saw that the handling of Table 4.

CONCLUSION

Undoped TiO_2 and 1.1, 3.9, 4.4 %wt Cr-doped TiO_2 have been successfully analyzed from powder x-ray diffraction data by qualitative and quantitative analysis using various method. Qualitative analysis was carried out with the identification of a phase or phases in the samples by comparison with "standard" patterns: COD and ICDD. In the undoped TiO_2, three titania phases: anatase, rutile, and brookite were obtained. In the 1.1 %wt Cr-doped TiO_2 is detected presenting two phases of TiO_2: anatase (major) and rutile (minor), while anatase (major), rutile (minor), chromium oxide (minor) and TiO_2-II (minor) present in the 3.9 %wt Cr-doped TiO_2 and the

4.4 %wt Cr-doped TiO_2. The quantitative phase analysis was calculated by comparing two methods: reference intensity ratio (RIR) and whole-pattern fitting (Rietveld analysis). The phase content of all samples calculated by RIR method are showed that the undoped TiO_2 consist of anatase (52.2%), rutile (25.1%) and brookite (22.7%) phases, while in the 1.1.%wt Cr-doped TiO_2 present anatase (87.0%) and rutile (13.0%). In the 3.9 %wt Cr-doped TiO_2 are detected anatase (91.0%), rutile (2.8%), CrO_2 (2.7%), and TiO_2-II (3.3%), while in the 4.4 %wt Cr-doped TiO_2 have contents anatase (96.0%), rutile (2.2%), CrO_2 (1.4%), and TiO_2-II (0.4%). The Rietveld refinement method was applied to extract structural parameters of undoped TiO_2 and a series of various %wt Cr-doped TiO_2 using the Fullprof program. The undoped TiO_2 consist of anatase (49.58%), rutile (38.39%) and brookite (12.03%), while in the 1.1 %wt Cr-doped TiO_2 present anatase (88.45%) and rutile (11.50%) phases. In the 3.9 %wt Cr-doped TiO_2 and in the 4.4 %wt Cr-doped TiO_2 respectively consist of 100% of anatase phase, while chromium dioxide and TiO_2-II phases can't be detected by Rietveld refinements. The undoped TiO_2 was refined in the crystal system and space group of anatase (tetragonal, $I4_1/amd$), rutile (tetragonal, $P4_2/mnm$) and brookite (orthorhombic, $Pbca$), while the 1.1.%wt Cr-doped TiO_2 was refined in the crystal system and space group of anatase (tetragonal, $I4_1/amd$), rutile (tetragonal, $P4_2/mnm$).

ACKNOWLEDGEMENT

REFERENCES

[1] Yang, L., Hakki, A., Wang, F., and Macphee, D.E., 2018, Photocatalyst efficiencies in concrete technology: The effect of photocatalyst placement, *Appl. Catal., B*, 222, 200–208.

[2] Chen, F., Zou, W., Qu, W., and Zhang, J., 2009, Photocatalytic performance of a visible light TiO2 photocatalyst prepared by a surface chemical modification process, *Catal. Commun.,* 10 (11), 1510–1513.

[3] Munusamy, S., Aparna, R.S.L., and Prasad, R.G.S.V., 2013, Photocatalytic effect of TiO_2 and the effect of dopants on degradation of brilliant green, *Sustainable Chem. Processes*, 4 (4), 1–4.

[4] Haghi, M., Hekmatafshar, M., Janipour, M.B., Gholizadeh, S.S., Faraz, M.K., Sayyadifar, F., and Ghaedi, M., 2012, Antibacterial effect of TiO_2 nanoparticles on pathogenic strain of *E. coli, IJABR*, 3 (3), 621–624.

[5] Visai, L., De Nardo, L., Punta, C., Melone, L., Cigada, A., Imbriani, M., and Arciola, C.R., 2011, Titanium oxide antibacterial surfaces in biomedical devices, *Int. J. Artif. Organs*, 34 (9), 929–946.

[6] Günes, S., Marjanovic, N., Nedeljkovic, J.M., and Sariciftci, N.S., 2008, Photovoltaic characterization of hybrid solar cells using surface modified TiO_2 nanoparticles and poly(3-hexyl)thiophene, *Nanotechnology*, 19 (42), 424009.

[7] Jasim, K., 2012, Natural dye-sensitized solar cell based on nanocrystalline TiO_2, *Sains Malaysiana*, 41 (8), 1011–1016.

[8] Grätzel, M., 2005, Solar energy conversion by dye-sensitized photovoltaic cells, *Inorg. Chem.*, 44 (20), 6841–6851.

[9] Yan, P., Wang, X., Zheng, X., Li, R., Han, J., Shi, J., Li, A., Gan, Y., and Li, C., 2015, Photovoltaic device based on TiO_2 rutile/anatase phase junctions fabricated in coaxial nanorod arrays, *Nano Energy*, 15, 406–412.

[10] Masuda, Y., and Kato, K., 2008, Liquid-phase patterning and microstructure of anatase TiO_2 films on SnO_2:F substrates using superhydrophilic surface, *Chem. Mater.*, 20 (3), 1057–1063.

[11] Kim, H.M., Seo, S.B., Kim, D.Y, Bae, K., and Sohn, S.Y., 2013, Enhanced hydrophilic property of TiO_2 thin film deposited on glass etched with O_2 plasma, *Trans. Electr. Electron. Mater.*, 14 (3), 152–155.

[12] Yang, L., Zhang, M., Shi, S., Lv, J., Song, X., He, G., and Sun, Z., 2014., Effect of annealing temperature on wettability of TiO_2 nanotube array films, *Nanoscale Res. Lett.*, 9 (1), 621.

[13] Hanaor, D.A.H., and Sorrell, C.C., 2011, Review of the anatase to rutile phase transformation, *J. Mater. Sci.*, 46 (4), 855–874.

[14] Baur, W.H., 1961, Atomabstéinde und Bindungswinkel im Brookit, TiO_2, *Acta Cryst.*, 14, 214–216.

[15] Dette, C., Pérez-Osorio, M.A., Kley, C.S., Punke, P., Patrick, C.E., Jacobson, P., Giustino, F., Jung, S.J., and Kern, K., 2014, TiO_2 anatase with a bandgap in the visible region, *Nano Lett.*, 14 (11), 6533–6538.

[16] Pascual, J., Camassel, J., and Mathieu, H., 1978, Fine structure in the intrinsic absorption edge of TiO_2, *Phys. Rev. B: Condens. Matter*, 18 (10), 5606–5614.

[17] Zallen, R. and Moret, M.P., 2006, The optical absorption edge of brookite TiO_2, *Solid State Commun.*, 137 (3), 154–157.

[18] Uyanga, E., Gibaud, A., Daniel, P., Sangaa, D., Sevjidsuren, G., Altantsog, P., Beuvier, T., Lee, C.H., and Balagurov, A.M., 2014, Structural and vibrational investigations of Nb-doped TiO_2 thin films, *Mater. Res. Bull.*, 60, 222–231.

[19] Suwarnkar, M.B., Dhabbe, R.S., Kadam, A.N., and Garadkar, K.M., 2014, Enhanced photocatalytic activity of Ag doped TiO_2 nanoparticles synthesized by a microwave assisted method, *Ceram. Int.*, 40 (4), 5489–5496.

[20] Lei, X.F., .Xue, X.X., and Yang, H., 2014, Preparation and characterization of Ag-doped TiO_2 nanomaterials and their photocatalytic reduction of Cr(VI) under visible light, *Appl. Surf. Sci.*, 321, 396–403.

[21] Avansi, W.Jr., Arenal, R., de Mendonça, V.R., Ribeiro, C., and Longo, E., 2014, Vanadium-doped TiO_2 anatase nanostructures: the role of V in solid solution formation and its effect on the optical properties, *CrystEngComm*, 16 (23), 5021–5027.

[22] Moradi, H., Eshaghi, A., Hosseini, S.R., and Ghani, K., 2016, Fabrication of Fe-doped TiO_2 nanoparticles and investigation of photocatalytic decolorization of reactive red 198 under visible light irradiation, *Ultrason. Sonochem.*, 32, 314–319.

[23] Zhao, Y., Li, C., Liu, X., Gu, F., Du, H.L., and Shi, L., 2008, Zn-doped TiO_2 nanoparticles with high photocatalytic activity synthesized by hydrogen–oxygen diffusion flame, *Appl. Catal., B*, 79 (3), 208–215.

[24] Peng, Y.H., Huang, G.F., and Huang, W.Q., 2012, Visible-light absorption and photocatalytic activity of Cr-doped TiO_2 nanocrystal films, *Adv. Powder Technol.*, 23 (1), 8–12.

[25] Dubey, R.S., and Singh, S., 2017, Investigation of structural and optical properties of pure and chromium doped TiO_2 nanoparticles prepared by solvothermal method, *Results Phys.*, 7, 1283–1288.

[26] Ould-Chikh, S., Proux, O., Afanasiev, P., Khrouz, L., Hedhili, M.N., Anjum, D.H., Harb, M., Geantet, C., Basset, J.M., and Puzenat, E., 2014, Photocatalysis with chromium-doped TiO_2: Bulk and surface doping, *ChemSusChem*, 7 (5), 1361–1371.

[27] Klug, H.P., and Alexander, L.E., 1954, X-Ray *Diffraction Procedures: For Polycrystalline and Amorphous Materials*, John Wiley & Sons., New York, 992.

[28] Snyder, R.L. and Bish, D.L., 1989, "Quantitative Analysis" in *Modern Powder Diffraction*, Bish, D.L., and Post, J.E., Eds., Mineralogical Society of America, Washington, D.C., 20, 101–144.

[29] Bish, D.L, and Howard, S.A., 1988, Quantitative phase analysis using the Rietveld method, *J. Appl. Crystallogr.*, 21, 86–91.

[30] Pecharsky, V., and Zavalij, P., 2009, Fundamentals of Powder Diffraction and Structural Characterization of Materials, 2nd Ed., Springer-Verlag US, 744.

[31] Rich, R., 2007, *Inorganic Reactions in Water*, 1st Ed., Springer-Verlag Berlin Heidelberg, 521.

[32] Rietveld, H.M., 1969, A profile refinement method for nuclear and magnetic structures, *J. Appl. Cryst.*, 2, 65–71.

[33] Roisnel, T., and Ridriguez-Carvajal, J., 2009, *Winplotr a graphic tool for powder diffraction*, CNRS-Lab. de Chimie du Solide et Inorganique Moléculaire Université de Rennes.

[34] Rodríguez-Carvajal, J., 2009, *An Introduction to the Program Fullprof*, Laboratoire Léon Brillouin (CEA-CNRS) CEA/Saclay, Gif sur Yvette, France.

[35] Shannon, R.D., 1976, Revised effective ionic-radii and systematic studies of interatomic distances in halides and chalcogenides, *Acta Cryst.*, A32, 751–767.